RSC Advances

ROYAL SOCIETY OF CHEMISTRY

www.rsc.org/advances

Growth of nanocrystalline CuS thin films at room temperature by a facile chemical deposition method

Reza Sahraei[a,*], Sajad Noshadi[a], Alireza Goudarzi[b]

[a]Department of Chemistry, University of Ilam, P.O. Box: 65315-516, Ilam, Iran

[b]Department of Polymer Engineering, Golestan University, Gorgan, Iran

*Corresponding author. Tel/ fax: +98 841 222 7022

E-mail address: r.sahraei@ilam.ac.ir & reza_sahrai@yahoo.com

Abstract

In this paper, we describe the preparation and characterization of the nanocrystalline CuS thin films, deposited via an inexpensive and facile chemical bath deposition method at room temperature. The X-ray diffraction analysis showed a hexagonal covellite structure. The average diameter of CuS nanocrystals was less than 10 nm in size, showing quantum size effects. FE-SEM images indicated that the substrate surface was covered by semispherical particles with the average size of about 100 nm. The influence of the deposition time on optical properties of the CuS films was studied. The optical band gap was estimated to be in the range between 2.35 eV and 2.50 eV, exhibiting considerable blue shift due to quantum size effects. The photoluminescence (PL) spectrum of the CuS films showed two characteristic bands, one narrow and intense band centered at 422 nm and another weak green band at 530 nm.

Keywords: Nanostructures; CuS thin films; Chemical deposition method; Optical properties

1. Introduction

In recent years, semiconductor nanostructures have been extensively studied, owing to their distinguished chemical, optical, and electronic properties, which depended on the size and

shape of the nanoparticles [1–3]. Nowadays, the solution phase approach has become a promising technique to prepare nanostructures [4, 5]. In the synthesis of nanoparticles in the solution phase, the control of nucleation and successive growth of particles are extremely sensitive to the synthetic parameters and play the important role in control of the size and the shape of nanostructures [6]. Copper sulfide (CuS) is an important semiconductor with unique electronic, optical, and chemical properties as well as potential applications in many fields such as thin films solar cells [7–9], electro-conductive coatings [10, 11], architectural glazing applications [12], and catalysis [13].

CuS thin films have been prepared by using various methods, including radio frequency reactive sputtering [14], electrodeposition [15], spray pyrolysis [16], successive ionic layer adsorption and reaction (SILAR) [17–19], and chemical bath deposition (CBD) [20–27]. Except CBD and SILAR, all mentioned methods need expensive and complex equipments as well as usually carry out at high temperatures and pressures. While CBD is a very facile and cost-effective method for preparation of high quality semiconductors thin films without the need for high temperatures and/or pressures as well as vacuum equipments. The CBD process carries out under ambient conditions and has the potential to replace expensive techniques such as vacuum evaporation, chemical vapor deposition and spray pyrolysis that are currently in use [28–31]. The CBD method also is one of the simple and economic techniques to deposit a wide variety of binary, ternary and composite thin films.

Some of the applied chemical methods for deposition of CuS thin films are based on the use of toluene and/or methanol as an organic solvent and ammonia as a complexing agent for copper ions [24-27, 32-35]. The toluene and ammonia are organic compounds with high volatility and toxicity and pose potential environmental and biological risks. In addition, some

studies on the deposition of CuS thin films were carried out at high temperatures [16, 32]. Recently, Chaki et al. [34] reported the preparation of the CuS thin films by chemical bath deposition and dip coating techniques at room temperature onto glass substrates using the mixed complexing agents of triethanolamine and ammonium hydroxide at pH =11.5. They reported the optical properties of the deposited CuS thin films in details. Safrani et al.[27] reported the chemically deposited CuxS thin films onto glass, Si and GaAs substrates using ammonium hydroxide and triethanolamine as the mixed compelexing agents at pH>12. Maji et al. [32] have reported the preparation of the CuS thin films by a metal organic deposition technique using toluene and methanol.

In this study, for deposition of CuS thin films, water and tri-sodium citrate were used as the solvent and the complexing agent, respectivly. Both water and tri-sodium citrates are nontoxic chemicals and renewable materials. Tri-sodium citrate is a tri-basic salt of citric acid which is used in foods, beverages as well as in various idustrials as buffering and emulsifying agents. Besides, tri-sodium citrate is one of the most common agents used in the synthesis of metallic and semiconductor nanostructures as a stabilizing and/or complexing agent [36, 37]. One advantage of our work compared to other works is that less chemical waste is generated and therefore the applied CBD method has been improved relatively in comparison to previous studies [24-27, 32-35]. In addition, in this work, deposition of nanocrystalline CuS thin films were carried out using a very facile CBD method at low temperature and short time. The deposited thin films were comprehensively characterized in terms of composition, structure, surface morphology, optical and photoluminescence properties.

2. Experimental

2.1. Preparation of CuS thin films

Commercial glass slides were used as substrates. Before film deposition, first the substrates were immersed in a sulphochromic acid solution, and then were washed thoroughly with double distilled water to remove any adhering impurities. The substrates were then dried in an oven at 90 °C for 1 h. The deposition solution was prepared by mixing 10 mL of 0.1 $molL^{-1}$ copper acetate monohydrate [$Cu(CH_3COO)_2.H_2O$] solution with 20 mL of 0.2 $molL^{-1}$ tri-sodium citrate dihydrate [$Na_3C_6H_5O.2H_2O$] solution as the complexing agent in a beaker. In the next step, 5 mL of 0.4 $molL^{-1}$ thioacetamide [CH_3CSNH_2] solution as source of S^{2-} ions was added to the initial mixed solution slowly. Finally, double distilled water was added to the reaction solution to make the volume close to 100 mL and the solution was stirred for 1 min for well mixing of the constituents. The pH of solution was 6.0. The prepared reaction solution was poured into a glass tank being used as a reaction vessel for the film deposition. Glass substrates were put vertically in the reaction vessel, and the glass tank was placed in a thermostat bath set at 25 ºC. After the desired deposition time, the deposited films were removed from reaction tank then washed with distilled water and dried in air at room temperature. Both sides of the glass substrates were coated with the films. Color of the deposition solution at the start was light blue, after the several minutes became green, and then shifted to dark-green.

2.2. Characterization of thin films

The atomic composition of the films was analyzed by energy-dispersive X-ray spectrometer (EDX) using an Oxford INCA II energy solid state detector. To investigate the presence of organic and/or other compounds in films, the Fourier transform infrared (FTIR) spectrum was obtained by a BRUKER EQUINOX 55 spectrometer in the range of 50–4000 cm^{-1} with a resolution of 0.5 cm^{-1}. X-ray diffraction (XRD) patterns were recorded with an automated Philips X'Pert X-ray diffractometer with CuKα radiation (40 kV and 30 mA) for 2θ values over

20–80º. The surface morphology of the CuS films were observed by field emission scanning electron microscopy (FE-SEM; Hitachi S-4200) under an acceleration voltage of 15 kV. The UV–vis spectra were obtained by means of a Perkin Elmer Lambda 25 spectrophotometer. The thin films thickness was measured by a Dektak^3 profilometer. The photoluminescence emission and excitation spectra of the films were measured using a Cary Eclipse fluorescence spectrophotometer. A xenon lamp was used for excitation of the CuS films in the UV region. All measurements were carried out at room temperature.

3. Results and discussion

3.1. Reaction mechanism

The CBD method is based on the formation of solid phase from a solution, which involves two steps as nucleation and particle growth. In the nucleation process, the clusters of molecules are formed under rapid decomposition of precursors and then particles combine to grow up to a certain thickness of the film by heterogeneous reactions on the substrate surface. [38]. In CBD technique, a soluble salt of the required metal is dissolved in an aqueous solution to release cations. Non-metallic element is provided by the suitable source compound. The anions and cations then react to form the compound. For deposition of nanocrystalline CuS thin films by CBD technique, copper acetate easily dissolves in water to form copper ions (Cu^{2+}) and thioacetamide decomposes according to reactions no.1-4 to give hydrosulfide ions (HS^-). Because constant of solubility products of CuS is very small ($K_{sp}=8\times10^{-37}$), the formation of CuS particles take place very rapidly. The fast formation of CuS particles leads to the fast growth of clusters as well as the aggregation of the particles, as a result a weak adherence of the CuS particles to the substrate. Therefore, in this study, tri-sodium citrate which used as a nontoxic

complexing agent (reaction no.5) plays a very important role to control the slow release of Cu^{2+} ions to react with HS^- ions (released from thioacetamide) and formation of the CuS thin films.

The chemistry of the CuS formation from the used reagents, during the deposition process, can be written as following [39]:

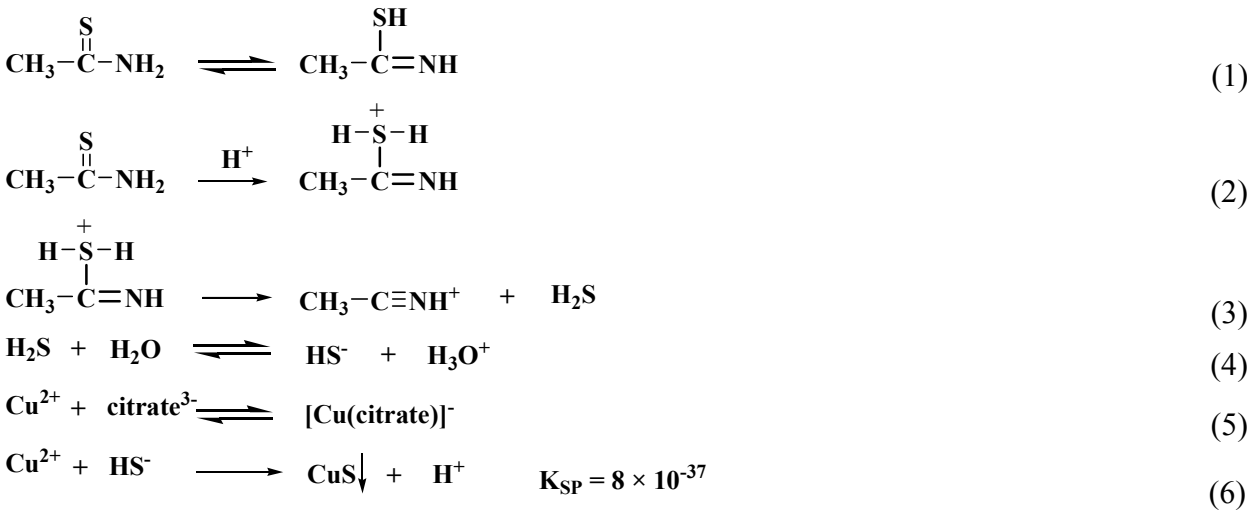

3.2. Deposition time effect on film thickness

Fig. 1 shows the variation of film thickness with deposition time. The deposition of CuS films was started onto the substrate glass by reaction of copper and sulfur ions, as explained in reaction mechanism section. The thickness of the CuS film increased with deposition time up to 30 min. The maximum thickness of 252 nm was obtained after a deposition period of 30 min. There was a continuous increase of film thickness with deposition time. With increasing deposition time up to 30 minutes, the film thickness increased with an approximately growth rate of 7.5 nm/min and reached to 225 nm. After 30 min, the noticeable change in films thickness was not observed.

3.3. Structural, compositional, and morphological characterizations

Fig. 2 shows the XRD pattern of the CuS film deposited on glass substrate at room temperature for 30 min. The standard XRD pattern for CuS (Joint Committee for Powder

Diffraction Standards, JCPDS card no. 78–2121) was given at the bottom of Fig. 2. The seven strong peaks observed in diffractogram at 2θ= 27,18, 29.45, 31.93, 32.75, 37.50, 48.65, and 60.20º are related to the lattice planes of (100), (102), (103), (006), (105), (110), and (116) the hexagonal phase of the CuS covellite structure, respectively [34]. No characteristic peaks were identified corresponding to any other phase of Cu_xS ($1 \leq x \leq 2$) except covellite CuS phase in the XRD pattern. This means that the pure covellite CuS thin films have been deposited by using chemical bath deposition method. The strong diffraction peaks suggest that the obtained CuS thin film is well crystalline in nature, while the as-prepared CuS films grown on Si and glass substrates using CBD method by Safrani et al. [27] had amorphous structure; even the annealed CuS films on glass substrates had amorphous structure. They improved the crystalinity of the prepared films on Si substrate by annealing at 200 ˚C for 2 hours. Although the annealed films at 200 °C were composed of a mixture of covellite (CuS) and digenite ($Cu_{1.8}S$) phases. Meanwhile, the prepared CuS films using CBD method by Cardoso et al., Chaki et al., and Lim et al. had amorphous structure [25, 34, 35].

On the basis of X-ray diffraction data, the lattice constants (*a* and *c*) for hexagonal structure of the CuS thin film were calculated from the interplanar distances (d_{hkl}) of all observed peaks in XRD pattern using the following equation [40]:

$$\frac{1}{d_{hkl}^2} = \frac{4}{3}\left(\frac{h^2 + hk + k^2}{a^2}\right) + \frac{l^2}{c^2} \tag{7}$$

and:

$$n\lambda = 2d_{hkl}\sin\theta_{hkl} \tag{8}$$

where θ_{hkl} is the corresponding diffraction Bragg angle, λ is X-ray wavelength of the CuKα1

radiation, and n is the diffraction order. For n= 1, from combining of two above equations we could easily derive the following expression:

$$Sin^2\theta_{hkl} = \frac{\lambda^2}{3}\left(\frac{h^2 + hk + k^2}{a^2}\right) + \frac{\lambda^2 l^2}{4c^2} \quad (9)$$

Eq. (9) was rearranged as follows:

$$Sin^2\theta_{hkl} = A(h^2 + hk + k^2) + Cl^2 \quad (10)$$

where: $A = \frac{\lambda^2}{3a^2}$, and $C = \frac{\lambda^2}{4c^2}$ (11)

According to Eq.(10), $\sin^2\theta_{hkl}$ depends linearly on h^2, k^2 and l^2 in hexagonal structure. On the basis of data for all peaks in the X-ray diffractogram of the CuS thin films deposited at room temperature for 30 min and using Eqs. (10) and (11), the values of the lattice constants were calculated. Then, in order to avoid from random and systematic errors on the measurement of θ_{hkl}, the lattice parameters values were also refined using multiple linear regression analysis. The refined values of the lattice parameters (*a* and *c*) were 3.789 and 16.360 Å, respectively. It is noticeable that the obtained lattice constants for the CuS thin film deposited at room temperature are in good agreement with the values reported in the literature (JCPDS card no. 78–2121, a = 3.791 Å and c = 16.342 Å).

As can be seen in Fig 2, the X-ray diffraction patterns for the CuS thin films deposited at room temperature are relatively broad. The overall broadening (β) of the XRD peaks is based on the three important factors. One of these factors is the approximate crystal diameter (L), another is the lattice strain (η), and the third factor is the instrumental broadening. In order to evaluate the contribution of each of these three factors, we start by expressing the overall broadening of the XRD peaks by the following relation [41, 42]:

$$\beta^2 \cos^2 \theta_{hkl} = A^2 + C^2 + \sin^2 \theta_{hkl}(B^2 - C^2) \quad (12)$$

In Eq. (12), $A = K\lambda/L$, where, K is the shape factor in spherical approximation which is approximately unity, λ is the wavelength of the used X-ray radiation, $B = 4\eta$, i.e. the stress-related broadening coefficient, while C is the instrumental factor contribution on the peak broadening. Thus, it is clear that when a linear least-square fit of $\beta^2 \cos^2 \theta_{hkl}$ is plotted versus $\sin^2 \theta_{hkl}$ a straight line with slope $(B^2 - C^2)$ and intercept $A^2 + C^2$ is obtained, as shown in Fig. 3. As can be seen in Fig. 3, it found out that the slope of this straight line is negative, which is expected when the stress-related broadening coefficient (B) value can be neglected. Thus, the lattice strain (η) contribution on the peaks broadening in the CuS thin films is very small. From the slope and the intercept of this straight line, we can calculate the A and C broadening coefficients values, respectively. The obtained A and C values for the CuS thin films deposited at room temperature were 1.67×10^{-2} and 8.36×10^{-3}, respectively. The instrumental-related broadening coefficient (C) value is smaller than that to the broadening coefficient related to the size of nanocrystals (A). This small value of the instrumental broadening coefficient indicates that the nanocrystals size factor plays important role on the broadening of X-ray diffraction peaks of the CuS films. Finally, according to these broadening coefficients values, the average diameter of the nanocrystals in the CuS thin films prepared at different deposition times were calculated and listed in Table 1.

A careful examination of the XRD pattern reveals that the intensity of (103) diffraction peak was obviously lower than that of the standard pattern. Also could be seen that the intensity of (110) diffraction peak is particularly strong, which indicates the preferential orientation growth along the (110) plane of the CuS film i.e. higher number of (110) planes are parallel to the substrate surface. Besides, the film deposited by CBD is under very low tensile strain along

the (110) plane parallel to the substrate surface. Furthermore, because of very small size of the CuS nanocrystals, the interplanar distance, d_{110}, of the planes parallel to the film surface (0.20658 nm) was less than the standard value for the bulk CuS powder (0.20775 nm). Therefore, according to the above results and review of the reported literatures, a possible mechanism of growth orientation of the CuS thin films can be proposed [43, 44]. The obtained ratio of the lattice constants (c/a) for the deposited hexagonal CuS was 4.32, which is greater than the ideal value for the hexagonal structure (1.633), implying that the {0001} facets have a surface energy lower than those of the $\{10\bar{1}0\}$ and $\{11\bar{2}0\}$ facets [45]. The larger area of the {0001} crystal surfaces can limit the exposure of other higher energy surfaces, reducing the total energy of the nanocrystals and resulting in the formation of the stable nanocrystals. It is believed that the Cu^{2+} cations react with the HS^- anions to form seeds that grow faster on the $(10\bar{1}0)$ and $(11\bar{2}0)$ planes and more slowly on the (0001) plane, forming small CuS nanocrystals.

Chemical composition of the prepared CuS thin films was analyzed by EDX, FTIR, and Raman spectroscopy. The EDX was used to quantitative analysis of the chemical composition of copper and sulfur in the CuS films. Fig. 4 shows the EDX spectrum of the CuS thin film deposited at room temperature for 30 min onto the silicon substrate. The average atomic ratio of Cu:S was 50.64:49.24, showing an excellent stoichiometry (Cu/S: 1.03) in the prepared CuS film.. Furthermore, one peak corresponding to silicon was observed which is related to its presence in the silicon substrate. In EDX spectrum, no peaks corresponding to other elements such as C and/or O were found. Therefore, on the basis of the obtained EDX analysis and XRD data, the films composition can be considered as the CuS covellite without other mixed phases.

In order to investigate the presence of organic compounds and/or other compounds such as CuO and $Cu(OH)_2$ as impurities in the CuS thin films, Fourier transform-infrared (FT-IR)

spectrum of the CuS film was obtained and studied. Cu–S band in the pure CuS powder is observed at 310 cm^{-1} [46]. Cu–O bond in the FT-IR spectrum of CuO powder have a medium peak at 425 cm^{-1} [46, 47]. The FT-IR spectrum of the prepared CuS film is shown in Fig. 5 (a). It consists of Cu–S peak at 312 cm^{-1} and revealed no peaks related to impurities except a very weak peak at 1620 cm^{-1} and a broad weak peak at 3200-3600 cm^{-1} that must be related to the stretching and bending modes of trace amounts of adsorbed water on the film [48, 49].

Raman spectroscopy is an effective method to investigate the material structure, so it is suitable for exploring the surface layer structure of the nanocrystalline thin films. The Raman spectrum of a typical CuS thin film is shown in Fig. 5 (b). A strong and sharp band at 478 cm^{-1} is observed which can be assigned to the S–S stretching mode (ν_{ss}) [50, 51]. The weak band at 951 cm^{-1} is probably due to the first overtone of the strongest band in the spectrum [52].

In order to study the surface morphology of the films, the deposited films were examined by field emission-scanning electron microscopy (FE-SEM). The FE-SEM images of the CuS thin films prepared at 30 min were shown in Fig. 6 at two different magnifications. As can be seen in Fig. 6, the prepared CuS film was homogeneous and consisted of small semispherical particles with an approximate diameter of 100 nm. The FE-SEM images also display the compactness and the surface uniformity of the films in comparison to other works [34, 35], are relatively good as well as the film well adherent to the glass substrates. The approximate size of particles is about 100 nm, whereas the average diameter of the nanocrystals estimated from the XRD pattern was about 10 nm, respectively. This suggests that each feature in the FE-SEM images is a polycrystalline particle.

3.4. Optical properties

Optical properties of the CuS thin films were studied by the fluorescence and optical absorption spectroscopy in the wavelength range of 300–800 nm. Transmittance and reflectance

spectra of the CuS films grown on glass substrate for 50 min at 25 °C were shown in Fig. 7. Initially, high transmittance was observed for the CuS thin films deposited at 10 min. As shown in Fig. 7, the transmittance of the prepared CuS film was decreased with deposition time. Also, the CuS thin films prepared at less deposition time (i.e. 10 min.) had higher transmittance in the visible region than those of the prepared at longer deposition time. This difference in transmittance value can be attributed to difference in thickness of the films prepared at different deposition time. The thicker films have been prepared at longer time and have lower transmittance, resulting higher absorbance in the visible region. These films have applicability as optical absorber layers in various industrials. Generally, the increase in thickness of the film as well as high compactness of the film grains are two the main factors for the intense decrease in transmittance values in the visible region.

The absorption coefficients (α) of the films have been calculated using the following relation valid for the near-edge absorption [53]:

$$\alpha = \frac{-1}{t}\ln\left\{\frac{T}{(1-R)^2}\right\} \tag{13}$$

where t is the thickness of the film, T and R are the transmission and reflectivity, respectively. The absorption coefficient (α) is related to the incident photon energy as follows [54]:

$$\alpha h\nu = k(h\nu - E_g)^m \tag{14}$$

where k is a constant, E_g is the separation between the valence and conduction bands (the band gap energy), and m is a value depending on the nature of the transition. The value of m is 1/2 for allowed direct transition. Also, h, and υ are the Planck constant, and frequency, respectively. The values of the band gap energy, E_g, were calculated from the optical absorption measurements by plotting $(\alpha h\upsilon)^2$ versus hυ. A typical Plot of $(\alpha h\upsilon)^2$ versus hυ for the CuS thin films deposited at

30 min was shown in Fig. 8. As can be seen $(\alpha h\upsilon)^2$ varies linearly with hυ above the energy gap. Accordingly, the energy gap is obtained by extrapolating the straight portion of the curve to zero absorption coefficients ($\alpha = 0$). The obtained band gap energies for the CuS thin films prepared at different deposition times are given in Table 1. As shown in Table 1, the band gap energy slightly shifts to a lower wavelength (higher energy) with decreasing deposition time. The band gap energy of the bulk covellite CuS is about 2.2 eV [55]. The blue shift in the band gap energy by an amount of about of 0.15-0.30 eV in the case of our chemically deposited CuS thin films, compared with the corresponding value of bulk material, probably is due to the quantum confinement effects, i.e., the CuS crystals present in the thin films matrix behave as three-dimensionally confined structures [56]. Furthermore, the existence of the CuS nanocrystals in the thin films form is in agreement with the average diameter of nanocrystals which is estimated on the basis of X-ray diffraction line broadening.

Room temperature photoluminescence (PL) spectrum of the CuS thin film is shown in Fig. 9. As can be seen in Fig. 9, two prominent PL emission peaks were observed under excitation of 370 nm. The first sharp emission peak appears at about 425 nm and the other at around 530 nm. In general, depending on the chemical composition and microstructure of the sample, copper sulphide films containing bulk crystallites exhibit broad emission bands at around 400-550 nm [57, 58]. A blue emission peak at 425 nm was also reported for the CuS nanowires by Zhang and Wong [59]. The peak shift and intensity are influenced by several parameters such as shape and size of the nanocrystals, which were controlled by synthesis conditions. The blue shift of this intense emission peak towards the lower wavelength region is attributed to the enhancement of the quantum confinement effect resulting from the decrease in the size of the CuS nanocrystals [16]. And also, the weak green emission peak at 530 nm can be

attributed to the surface defects in the CuS crystal lattice. The chemically deposited CuS films may have some nonstoichiometric structure with defects [59]. The green emission is in good agreement with the PL spectrum of the nanocrystalline CuS thin film as was observed previously by Mukherjee et al. [60].

4. Conclusion

Good quality CuS thin films in view point of particle compactness, thickness, structure, optical absorbance, and light emission were successfully fabricated by a very facile chemical bath deposition method at low temperature using tri-sodium citrate as a non-toxic and environment friendly compelexing agent instead of ammonia for copper ions. The prepared CuS thin films had good adherence to the substrate. The XRD and FT-IR analysis of the prepared CuS thin films revealed no peaks related to impurities. FE-SEM images showed a homogenous and dense deposition of the CuS particles all over the substrate with the average size of 100 nm.

The PL spectrum confirmed the blue shift around 425 nm is attributed to the quantum confined effect as a result of the formation of the nanosized CuS crystals. In addition, optical measurements revealed that the CuS thin films had high absorbance in the visible region, indicating that their applicability for low cost absorber layer in thin film solar cell materials.

References

[1] J. Park, J. Joo, S.G. Kwon, Y. Jang, T. Hyeon, Angew. Chem. Int. Ed. 46 (2007) 4630–4660.

[2] C. Burda, X.B. Chen, R. Narayanan, M.A. El-Sayed, Chem. Rev. 105 (2005) 1025–1102.

[3] Y.F. Zhu, D.H. Fan, W.Z. Shen, Langmuir 24 (2008) 11131–11136.

[4] A.L. Rogach, T. Franzl, T.A. Klar, J. Feldmann, N. Gaponik, V. Lesnyak, A. Shavel, A. Eychmuller, Y.P. Rakovich, J.F. Donegan, J. Phys. Chem. C 111 (2007)14628–37.

[5] R. Sahraei, M. Nosrati, A. Danesfar, S. Abbasi, M.H. Majles Ara, Mater. Lett. 68 (2012) 153–156.

[6] Y. Xia, Y. Xiong, B. Lim, S.E. Skrabalak, Angew. Chem. Int. Ed. 48 (2009) 60–103.

[7] Z. Liu, J. Han, L. Han, K. Guo, Y. Li, T. Cui, B. Wang, X. Liang, Mater. Chem. Phys. 141 (2013) 804–809.

[8] S.S. Kalanur, S.Y. Chae, O.S. Joo, Electrochimica Acta 103 (2013) 91–95.

[9] P.J. Sebastian, O. Gomez-Daza, J. Campos, L. Banos, P.K. Nair, Sol. Energy Mater. Sol. Cells 32 (1994) 159–168.

[10] S.B. Gadgil, R. Thangaraj, J.V. Lyer, A.K. Sharma, B.K. Gupta, O.P. Agnihotri, Sol. Energy Mater. Sol. Cells 5 (1981) 129–140.

[11] S. Lindroos, A. Arnold, M. Leskelä, Appl. Surf. Sci. 158 (2000) 75–80.

[12] A. Bollero, M. Grossberg, B. Asenjo, M.T. Gutiérrez, Surf. Coat. Tech. 204 (2009) 593–600.

[13] Z. Hai, J. Huang, H. Remita, J. Chen, Mater. Lett. 108 (2013) 304–307.

[14] Y.B. He, A. Polity, I. Osterreicher, D. Pfisterer, R. Gregor, B.K. Meyer, M. Hardt, Physica B 308–310 (2001) 1069–1073.

[15] S.S. Dhasade, J.S. Patil, J.H. Kim, S.H. Han, M.C. Rath, V.J. Fulari, Mater. Chem. Phys. 137 (2012) 353–358.

[16] M. Adelifard, H. Eshghi, M.M. Bagheri Mohagheghi, Appl. Surf. Sci. 258 (2012) 5733–5738.

[17] M.A. Yildirim, A. Ateş, A. Astam, Physica E 41 (2009) 1365–1372.

[18] S.D. Sartale, C.D. Lokhande, Mater. Chem. Phys. 65 (2000) 63–67.

[19] Y. Shi, F. Xue, C. Li, Q. Zhao, Z. Qu, X. Li, Appl. Surf. Sci. 258 (2012) 7465–7469.

[20] E. Güneri, A. Kariper, J. Alloys Compd. 516 (2012) 20–26.

[21] Y. Lu, X. Meng, G. Yi, J. Jia, J. Colloid Interface Sci. 356 (2011) 726–733.

[22] Y. Lu, G. Yi, J. Jia, Y. Liang, Appl. Surf. Sci. 256 (2010) 7316–7322.

[23] Y. Lu, S. Liang, M. Chen, J. Jia, J. Colloid Interface Sci. 332 (2009) 32–38.

[24] P.K. Nair, V.M. Garcia, A.M. Ferndndez, H.S. Ruiz, M.T.S. Nair, J. Phys. D: Appl. Phys. 24 (1991) 441–449.

[25] J. Cardoso, O. GomezDaza, L. Ixtlilco, M.T.S. Nair, P.K. Nair, Semiconduct. Sci. Technol. 16 (2001) 123–127.

[26] A. A. Sagade, R. Sharma, Sens. Actuators B 133 (2008) 135–143.

[27] T. Safrani, J. Jopp, Y. Golan, RSC Adv. 3 (2013) 23066–23074.

[28] A. Goudarzi, G. Motedayen Aval, S.S. Park, M.C. Choi, R. Sahraei, M. Habib Ullah, A. Avane, C.S. Ha, Chem. Mater. 21 (2009) 2375–2385.

[29] J. Aguilar-Hernandez, G. Contreras-Puente, A. Morales-Acevedo, O.Vigil-Galan, F. Cruz-Gandarilla, Semicond. Sci. Technol. 18 (2003) 111–114.

[30] S.M. Pawar, B.S. Pawar, J.H. Kim, O.S. Joo, C.D. Lokhande, Curr. Appl. Phys. 11 (2011) 117–161.

[31] R. Sahraei, S. Darafarin, Spectrochim. Acta Part A 149 (2015) 941–948.

[32] S.k. Maji, N. Mukherjee, A.K. Dutta, D.N. Srivastava, P. Paul, B. Karmakar, A. Mondal, B. Adhikary, Mater. Chem. Phys. 130 (2011) 392–397.

[33] Y.T. Nien, I.G. Chen, J. Alloys Compd. 471 (2009) 553–556.

[34] S.H. Chaki, M.P. Deshpande, J.P. Tailor, Thin Solid Films 550 (2014) 291–297.

[35] I. Lim, D.Y. Lee, S.A. Patil, N.K. Shrestha, S.H. Kang, Y.C. Nah, W. Lee, S.H. Han, Mater. Chem. Phys. 148 (2014) 562–568.

[36] N.G. Bastús, F. Merkoçi, J. Piella, V. Puntes, Chem. Mater. 26 (2014) 2836–2846.

[37] R. Sahraei, A. Daneshfar, A Goudarzi, S. Abbasi, M.H. Majles Ara, F. Rahimi, J. Mater. Sci: Mater. Electron. 24 (2013) 260–266.

[38] V.R. Shinde, C.D. Lokhande, R.S. Mane, S.H. Han, Appl. Surf. Sci. 245 (2005) 407–413.

[39] K. Y. Rajpure, A. L. Dhebe, C. D. Lokhande, C. H. Bhosale, Mater. Chem. Phys. 56 (1998) 177–183.

[40] C. Suryanarayana, M. G. Norton, X-Ray Diffraction, Plenum Press, New York, 1998.

[41] B. Pejova, I. Bineva, J. Phys. Chem. C 117 (2013) 7303–7314.

[42] J. Mazher, A.K. Shrivastav, R.V. Nandedkar, R.K. Pandey, Nanotechnology 15 (2004) 572–580.

[43] K.J. Wang, G.D. Li, J.X. Li, Q. Wang, J.S. Chen, Cryst. Growth Des. 7 (2007) 2265–2267.

[44] M. Xin, K.W. Li, H. Wang, Appl. Surf. Sci. 256 (2009) 1436–1442.

[45] Z.A. Matysina, Mater. Chem. Phys. 60 (1999) 70–78.

[46] N.T. Akinchan, D.X. West, Y.H. Yang, M.M. Salberg, T.L. Klein, Transition Met. Chem. 20 (1995) 481–484.

[47] S.P. Sovilj, G. Vuckovic, V.M. Leovac, D.M. Minic, Polish J. Chem. 74 (2000) 945–954.

[48] S. Lindroos, T. Kannainen, M. Leskela, Mater. Res. Bull. 32 (1997)1631–1636.

[49] F. Wegmuller, J. Colloid Interface Sci. 116 (1987) 312–333.

[50] M. Ishi, K. Shibata, H. Nozaki, J. Solid State Chem.105 (1993) 504–511.

[51] C.G. Munce, G.K. Parker, S.A. Holt, G.A. Hope, Colloids Surf. A 295 (2007) 152–158.

[52] B. Minceva-Sukarova, M. Najdoski, I. Grozdanov, C. Chunnilall, J. Mol. Struct. 410–411 (1997) 267–270.

[53] D.S. Koktysh, J.R. McBride, S.J. Rosenthal, Nanoscale. Res. Lett. 2 (2007) 144–148.

[54] A. Goudarzi, G. Motedayen Aval, R. Sahraei, H. Ahmadpoor, Thin Solid Films 516 (2008) 4953–4957.

[55] K. Mageshwari, S.S. Mali, T. Hemalatha, R. Sathyamoorthy, P.S. Patil, Prog. Solid State Chem. 39 (2011) 108–113.

[56] A. Goudarzi, A.D. Namghi, C.S. Ha, RSC Adv. 4 (2014) 59764–59771.

[57] F. Zhang, S. S. Wong. Chem. Mater. 21 (2009) 4541–4554.

[58] Y. Du, Z. Yin, J. Zhu, X. Huang, X. Wu, Z. Zeng, Q. Yan, H. Zhang, Nat. Commun. 3 (2012) 1177.

[59] M.T.S. Nair, M.C. Lopez, O. GomezDaza, P.K. Nair, Semicond. Sci. Technol. 18 (2003) 755–779.

[60] N. Mukherjee, A. Sinha, G. G. Khan, D. Chandra, A. Bhaumik. Materials Research Bulletin 46 (2011) 6–11.

Figures caption:

Fig. 1. Variation of the film thickness versus deposition time of the CuS thin film deposited on glass substrate at 25 °C.

Fig. 2. X-ray diffraction pattern of the as-deposited CuS thin film at 25 °C for 30 min.

Fig. 3. : Plot of $\beta^2 \cos^2\theta$ versus $\sin^2\theta$ for the CuS thin film deposited at 25 °C for 30 min.

Fig. 4. EDX spectrum of a typical CuS thin film deposited on silicon substrate at 25 °C for 30 min.

Fig. 5. (a) The FT-IR transmittance and (b) the Raman spectra of a typical CuS thin film deposited at 25 °C for 30 min.

Fig. 6. Typical low-magnification (a) and high-magnification (b) SEM images of the CuS thin film prepared at 25 °C for 30 min.

Fig. 7. UV-visible transmission and reflection spectra of the CuS thin films prepared at different deposition times.

Fig. 8. Typical Plot of $(\alpha h\upsilon)^2$ versus $h\upsilon$ for the CuS thin films deposited at 25 °C for 30 min.

Fig. 9. PL spectrum of a typical CuS thin film deposited at 25 °C for 30 min.

Table 1. The film thickness, the band gap energy, and the nanocrystals size values for the CuS thin films deposited at different deposition times

Deposition time (min.)	Film thickness (nm)	Band gap energy (eV)	Nanocrystals size (nm)
10	83	2.55	7.6
15	130	2.47	8.2
20	184	2.44	8.5
25	238	2.41	8. 8
30	245	2.35	9.2
40	243	2.36	9.6
50	239	2.36	9.5

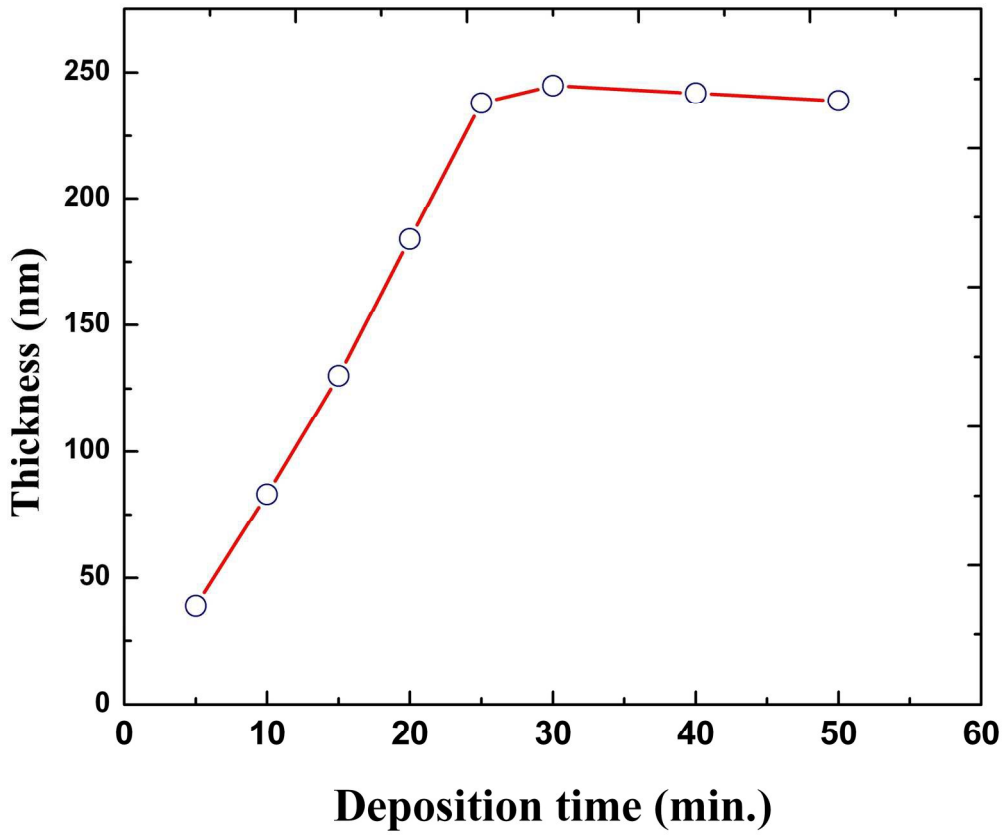

Fig.1
180x150mm (300 x 300 DPI)

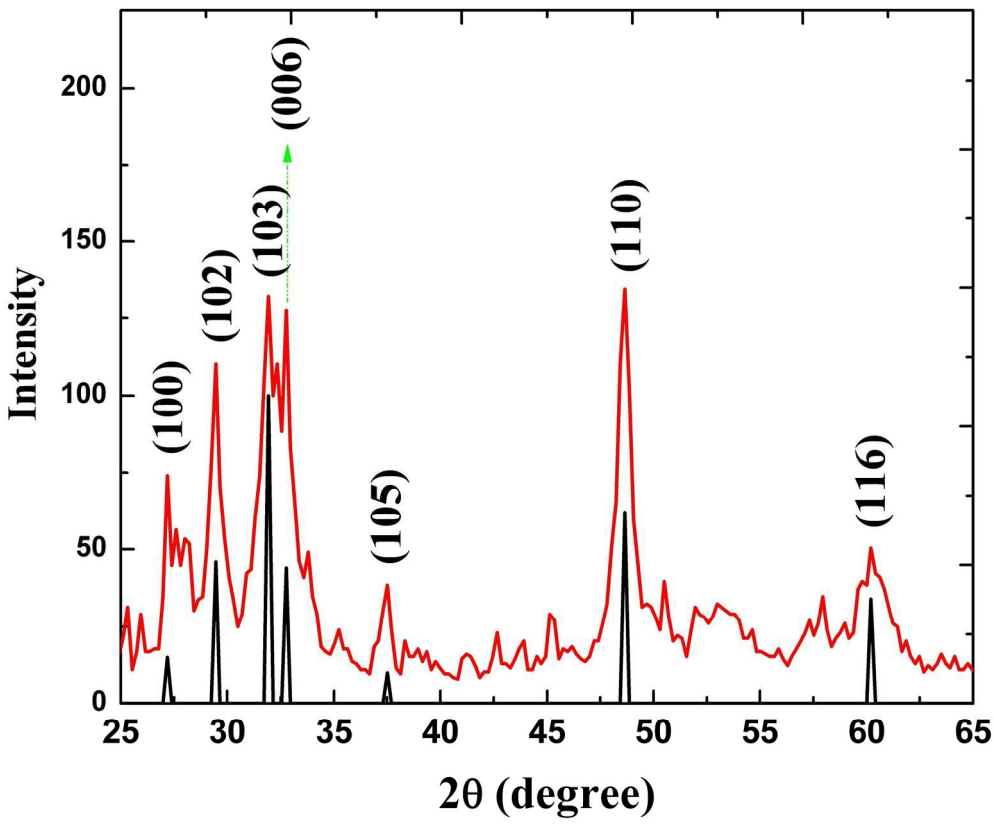

Fig.2
178x146mm (300 x 300 DPI)

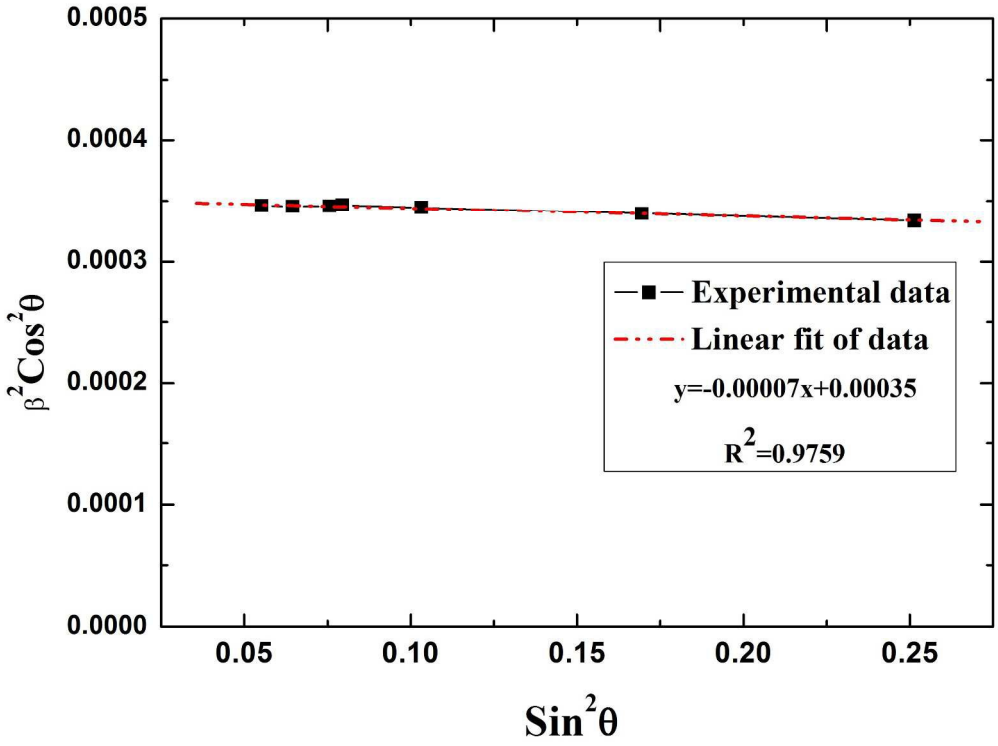

Fig.3
237x176mm (300 x 300 DPI)

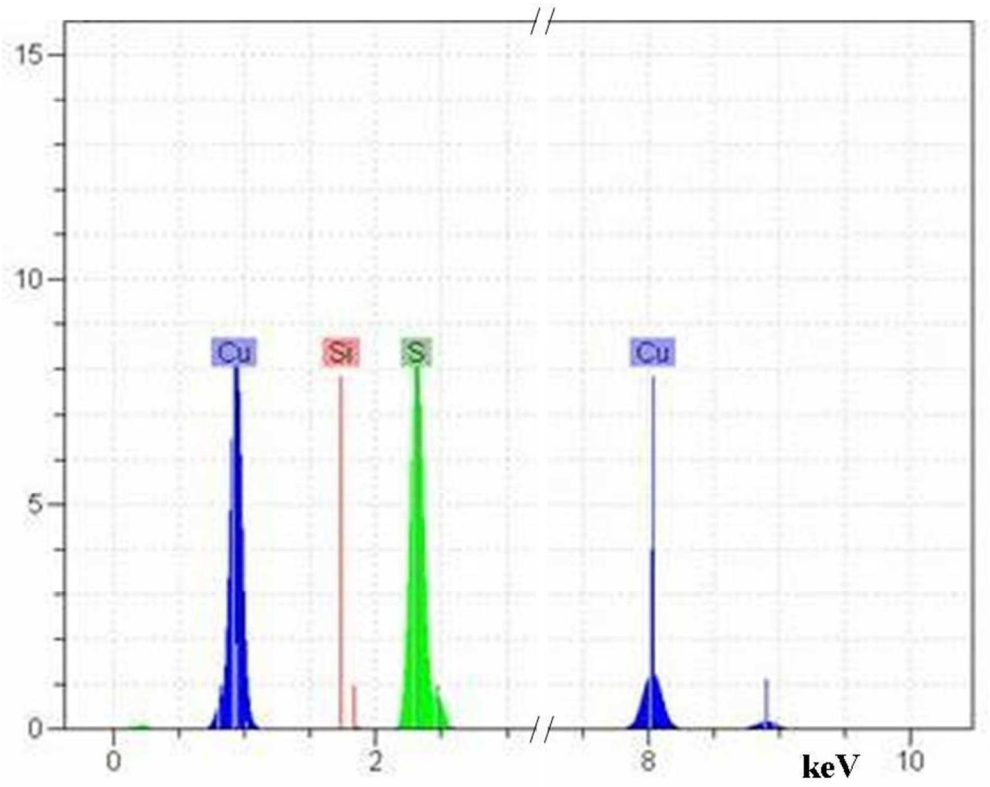

243x190mm (96 x 96 DPI)

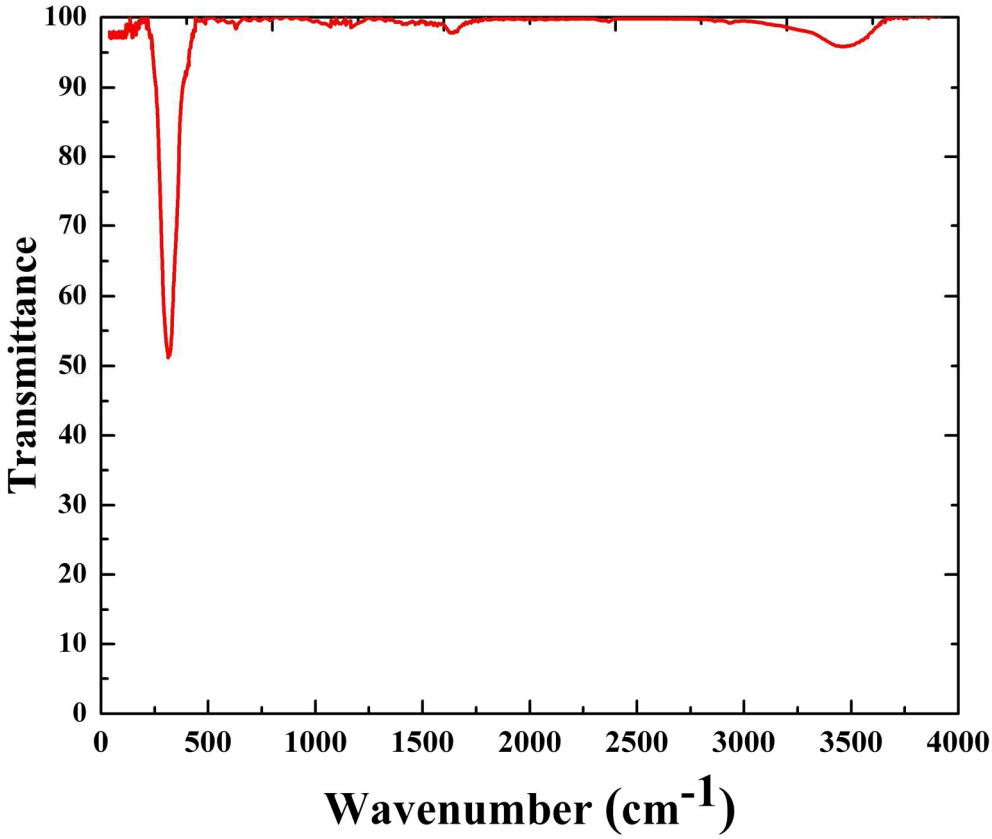

Fig.5a
182x153mm (300 x 300 DPI)

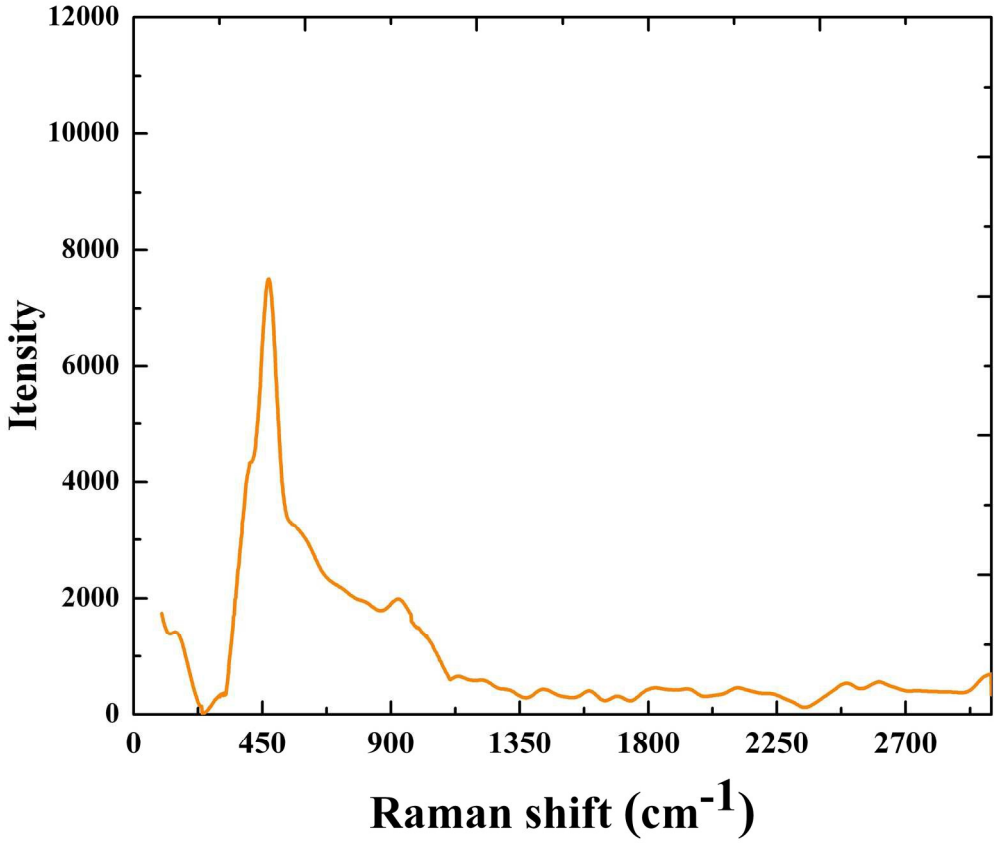

Fig.5b
182x155mm (300 x 300 DPI)

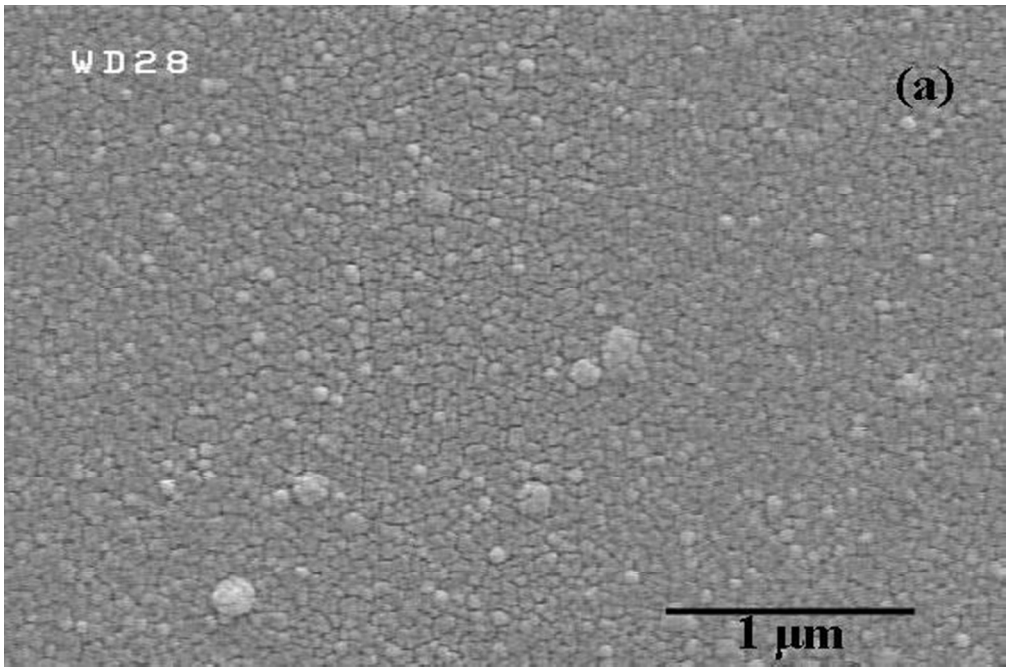

Fig.6a
168x111mm (96 x 96 DPI)

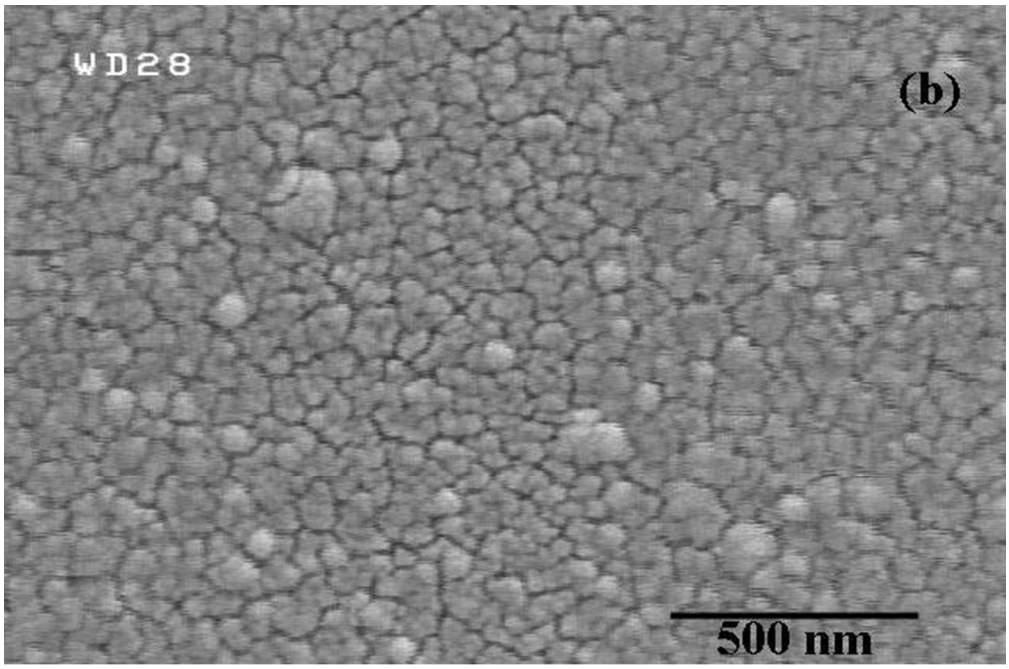

Fig.6b
169x111mm (96 x 96 DPI)

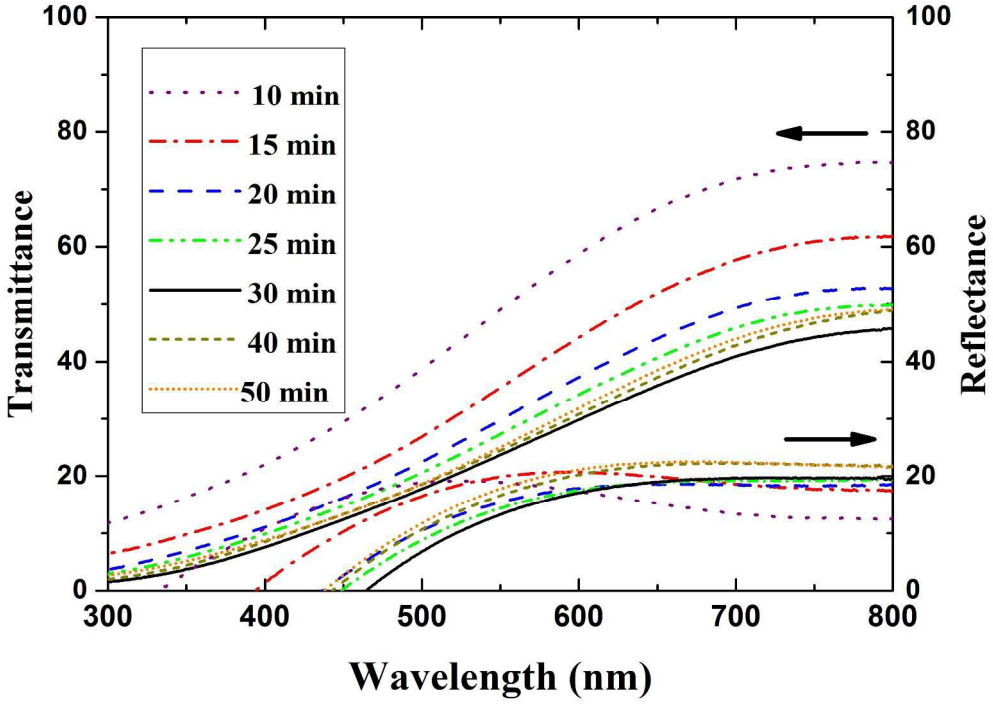

Fig.7
251x177mm (300 x 300 DPI)

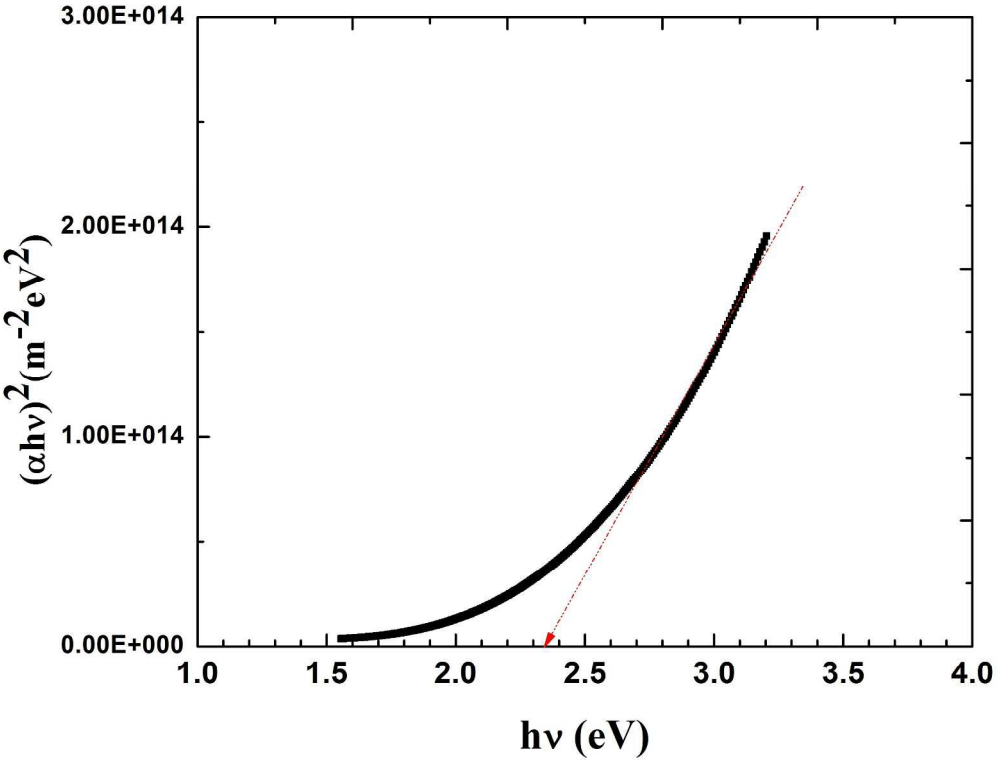

Fig.8
246x188mm (300 x 300 DPI)

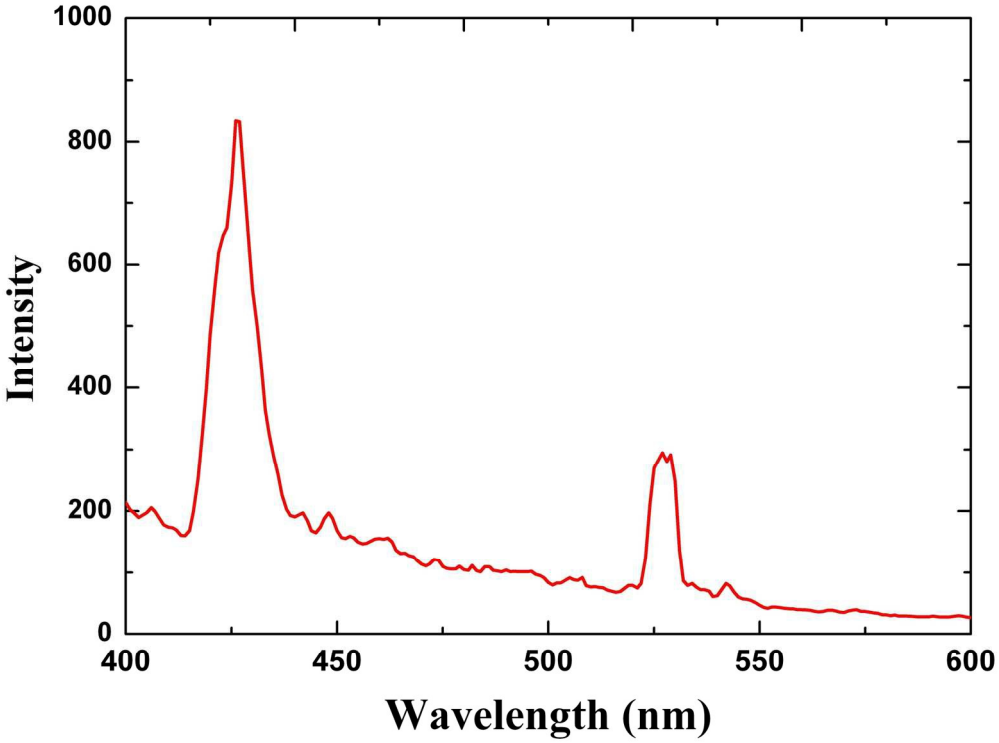

Fig.9
160x121mm (300 x 300 DPI)